Chemical Engineering Journal 445 (2022) 136513

Contents lists available at ScienceDirect

Chemical Engineering Journal

journal homepage: www.elsevier.com/locate/cej

Plant-based amyloids from food waste for removal of heavy metals from contaminated water

Wei Long Soon [a,b], Mohammad Peydayesh [b], Raffaele Mezzenga [a,b,c,*], Ali Miserez [a,d,*]

[a] Center for Sustainable Materials (SusMat), School of Materials Science and Engineering, Nanyang Technological University, 639798, Singapore
[b] ETH Zurich, Department of Health Sciences and Technology, 8092 Zurich, Switzerland
[c] ETH Zurich, Department of Materials, Wolfgang-Pauli-Strasse 10, 8093 Zurich, Switzerland
[d] School of Biological Sciences, Nanyang Technological University, 60 Nanyang Drive, 637551, Singapore

ARTICLE INFO

Keywords:
Sustainability
Waste Management
Recycling
Water Treatment
Protein Processing
Circular Economy

ABSTRACT

Water pollution is one of the major global threats brought about by industrial, agricultural, and any other anthropogenic activity. Heavy metals represent a large group of water pollutants that can accumulate in the human body, causing cancer and mutagenic diseases. Technologies currently used to treat polluted wastewaters of heavy metals employ chemical, ion-exchange, and membrane purification methods. However, these techniques are energy-intensive due to high pressure and power requirements for membrane-based technologies, or highly selective, as in ion-exchange resins, making drinking water less affordable in developing countries. In this study, plant amyloid-carbon membranes consisting of sunflower and peanut amyloid fibrils were fabricated through a green and sustainable process and were used to remove toxic heavy metal pollutants to drinkable standards with negligible energy consumption. Protein-rich sunflower and peanut meals serve as low-cost raw materials, from which proteins were extracted, isolated, and self-assembled into functional amyloid fibrils for heavy metal removal. These amyloid fibrils were incorporated into hybrid carbon/amyloid membranes and used to filer Pt-, Cr-, and Pb-containing water to produce water of drinkable standards containing < 10 ppb heavy metals. This process can easily be upscaled due to its simplicity and minimal use of chemical reagents, pointing towards the future of low-cost yet efficient water treatment technologies.

1. Introduction

Water contamination is one of the most critical environmental pollution affecting the Earth ecosystem. Millions of people suffer from the adverse effects of water pollution, especially in regions without proper and adequate water sanitation. One major perpetrator is heavy metals contamination from industrial wastewaters [1] such as mining activities, electroplating, and textile industries. Effluents containing high levels of heavy metals discharged into water bodies negatively affect not just aquatic life, but also humans when drawing water from these water bodies, leading to heavy metal poisoning, diseases and death.

Conventional methods to treat heavy metals from wastewater include chemical precipitation, ion-exchange, electrodialysis, and membrane processes [2,3]. However, these technologies suffer from several drawbacks such as secondary pollution, regeneration, and energy input, all of which increase the cost of clean drinking water while lacking long-term sustainability [1,4]. Adsorption technologies have drawn increased interest in recent years due to the wider variety of available materials along with their simple operation, which adequately address more sustainable and greener demands [5,6]. Notably, these efforts have turned towards materials from natural resources such as clay, minerals, polysaccharides, and biological materials, which possess a plethora of functional chemical groups for heavy metal adsorption. Moreover, these materials are either naturally abundant or derived from waste and biodegradable, thus enhancing the sustainability factor of water treatment [7]. Nevertheless, there are still several drawbacks with adsorption technologies, such as the high energetic cost associated with the production of adsorbents, secondary pollution from regeneration, and varying selectivities dependent on the adsorbent used [8]. As a result, these factors may not significantly lower the cost and environmental impact of adsorption technologies compared to conventional

* Corresponding authors at: Center for Sustainable Materials (SusMat), School of Materials Science and Engineering, Nanyang Technological University, 639798, Singapore and ETH Zurich, Department of Health Sciences and Technology, 8092, Zurich, Switzerland.
E-mail addresses: raffaele.mezzenga@hest.ethz.ch (R. Mezzenga), ali.miserez@ntu.edu.sg (A. Miserez).

https://doi.org/10.1016/j.cej.2022.136513
Received 2 February 2022; Received in revised form 17 April 2022; Accepted 18 April 2022
Available online 30 April 2022

water treatment methods. Hence, there is a critical need to further reduce the cost and improve the sustainability factor of heavy metal removal through adsorption.

Among biological materials, proteins serve as a promising tool for heavy metal adsorption due to the multitude of functional groups from different amino acids that exhibit metal-binding capability [9]. In recent years, amyloid fibrils self-assembled from whey proteins, such as β-lactoglobulin, have shown an unprecedented ability for the purification of heavy metals-polluted wastewater [10–15]. Owing to the exposure of metal-binding amino acids on the surface of high aspect ratio protein fibrils [11], hybrid amyloid-based membranes have been demonstrated to feature more than 99% removal efficiency for a wide variety of heavy metals and radioactive compounds commonly found in wastewater, making protein amyloid fibrils a highly attractive material for heavy metal adsorption [16]. However, while the low-cost of β-lactoglobulin hybrid membranes makes them a sustainable technology for water purification, the shift from conventional animal farming towards sustainable practices could potentially increase whey prices in the near future [17], spurring the need to seek out lower cost alternative protein sources to fabricate amyloid-based membranes.

Plant proteins represent an abundant source of food proteins that can be sustainably valorized from food and agricultural wastes. While earlier reports have shown that plant proteins – such as pure soy [18,19] and zein proteins [20]– are able to remove heavy metals, these proteins have not yet been considered in the superior amyloid nanofibril state. Furthermore, they still have some commercial relevance in the food industry [21]. The production of commercial household vegetable oils from oilseed crops generates byproducts of oilseed meals comprising of 30–40% proteins [22–24]. Sunflower and peanut meals are among the most produced vegetable oils but have yet to find commercial applications, and are mainly used as animal fodder due to a lack of essential amino acids along with the allergenic nature of peanut proteins, which makes it unsuitable for human consumption. Considering the high volume generated by these protein-rich wastes [25], sunflower and peanut meals hence serve as potential protein alternatives towards the value-adding application of water purification.

In this study, plant-based amyloid fibrils were used as efficient heavy metal adsorbents for water purification. Sunflower and peanut proteins were extracted and isolated from their respective kernels and transformed into amyloid fibrils, with a systematic study of fibrillization conditions. Their heavy metal-binding capabilities and hybrid membrane performance were demonstrated by efficiently removing three heavy metals from water solutions, namely platinum (Pt), chromium (Cr) and lead (Pb). The results demonstrate the valorization of a low-cost industrial byproduct into high-value filter membranes, providing drinkable waters that meet world health organization (WHO) heavy metal standards via a simple operation with little to no power consumption. Furthermore, the whole process can be easily upscaled at minimal cost, potentially enabling to re-process waste streams for further applications and fully exploiting the different constituents of industrial food wastes.

2. Materials

Sunflower seeds and peanut kernels were purchased from local supermarkets. Activated Carbon, Ethylenediaminetetraacetic acid, Thiazole Orange, Lead (II) acetate (99.999% trace metals basis), Gold (III) chloride (99.995% trace metals basis), Nickel (II) sulfate (99.99% trace metals basis), Copper (II) chloride (99.999% trace metals basis), and Chromium trioxide (99.99% trace metals basis) were purchased from Sigma-Aldrich. Hydrogen hexachloroplatinate was purchased from TCI Chemicals, Singapore.

3. Methods

3.1. Meal protein extraction and isolation

Sunflower seeds and peanut kernels were screw-pressed to extract their oils. The residual masses obtained are termed meals and were blended into smaller flakes. Meals were defatted with n-hexane (1:5 w/v ratio) five times for one-hour each and were air-dried overnight. Sunflower and peanut meals were extracted twice with 1.3 M and 1 M NaCl, respectively, at a ratio of 1:10 w/v for one hour. The suspensions were centrifuged at 10,000 rpm for 10 min and the supernatant containing the extracted proteins was filtered through a filter paper to remove residual particles. The protein solution was concentrated using a tangential flow filtration setup with a molecular weight (MW) cutoff of 100 kDa (Sartorius Vivaflow 200) to one fourth of the original volume. Each concentrated protein solution was then precipitated by a 9:1 (v/v) dilution into cold water. The precipitated protein was let to settle, after which the mixture was decanted to obtain crude proteins, which were then freeze-dried. The crude proteins were dissolved in 10% (w/v) NaCl, centrifuged to remove insoluble matter, and precipitated by adjusting to pH 3. The isolated proteins were then washed and freeze-dried.

3.2. Sodium dodecyl sulfate polyacrylamide gel electrophoresis (SDS-PAGE)

Freeze-dried protein isolates were prepared at 2 mg/ml dissolved in 8 M urea. 10 μL Laemmli buffer was added to 10 μL protein solution. To reduce the disulfide bonds, an additional 1 μL of 1 M TCEP was added. SDS-PAGE was performed with a homogenous 12% gel using MW markers 10 to 250 kDa at 150 V for 65 min. The gel was then fixed with MeOH/EtOH/AcOH solution and subsequently stained with Coomassie Blue Silver Staining buffer. Gel images were analyzed using the GelAnalyzer software.

3.3. Amyloid fibril formation

Sunflower and peanut protein isolates were dissolved in water, adjusted to pH 2 with 6 M HCl and centrifuged at 10,000 rpm for 10 min to remove insoluble matter. Sunflower and peanut protein solutions were heated at 100 °C and 90 °C, respectively, for 24 h in an oil bath to induce amyloid fibril formation, followed by ice quenching to stop the reaction. The Bradford assay was performed prior the heat treatment using bovine serum albumin (BSA) as a standard to determine the protein concentrations. To determine the optimal heat treatment duration for amyloid fibril formation, 100 μL of heated protein solutions sampled at different time intervals were diluted twice with water, after which thiazole orange was added to a final concentration of 10 μM [26,27]. The solutions were excited with a wavelength of 421 nm and the fluorescence emission was measured at a wavelength of 455 nm (Tecan Spark). Fluorescent intensities were normalized to the intensities measured at 0 h.

3.4. Amino acid analysis

Triplicates of 10 μL sunflower and peanut amyloid fibril solutions were hydrolyzed in 500 μL of 6 M HCl solution containing 0.5% phenol under vacuum at 110 °C for 24 h. Solvents were removed by centrifugal vacuum and the hydrolysates were washed twice with water. Dried samples were kept at −20 °C prior to analysis. For analysis, hydrolyzed samples (0.5 mg/ml) were dissolved in a pH 2.2 citrate buffer. Composition analysis was performed with an amino acid analyzer (Sykam S433, Germany) using a ninhydrin buffer system.

3.5. Atomic Force microscopy

20 μL of fivefold-diluted amyloid fibril solution was deposited on a

freshly cleaved mica surface and incubated for 3 min. The surface was then washed with Milli-Q water and dried under nitrogen. Imaging with an Atomic Force Microscope (AFM) (NX10, Park Systems) was performed in non-contact mode with a scan rate of 1 Hz and scan size of 10 by 10 μm.

3.6. Electron microscopy characterization

Amyloid fibrils were diluted to 0.2 wt%, prepared on a copper grid and stained with uranyl acetate before imaging using transmission electron microscopy (TFS Morgagni 268) at an operating voltage of 100 kV. Pristine amyloid fibril membranes filtered with heavy metal solutions were carbon coated and imaged with scanning electron microscopy (FEI Magellan 400) equipped with EDX (EDAX Octane Super) at an operating voltage of 5 kV.

3.7. Membrane fabrication and heavy metal filtration

Amyloid-carbon membranes were fabricated by mixing a 2 wt% amyloid fibril solution with 10 wt% activated carbon. To make a 10 wt% amyloid-90% carbon membrane, 500 μL of 2 wt% amyloid fibril solution was mixed with 1 mL of 10 % (w/v) activated carbon solution. The solution was deposited on a 0.22 μm cellulose membrane and the solvent was removed by vacuum filtration. Heavy metal solutions were prepared by dilution from stock solutions. Filtration studies were conducted with both single and 10-cycle filtrations of 10 mL heavy metal solutions, after which the heavy metal ion concentrations in the permeate were analyzed with Induced Coupled Plasma-Optical Emission Spectroscopy (ICP-OES) (Optima 8000, Perkin Elmer). Permeates from 10-cycle filtration studies were measured with Induced Coupled Plasma Spectroscopy – Mass Spectroscopy (ICP-MS) (Elan DRC-e, Perkin Elmer). All experiments were performed in triplicates. Membrane efficiencies (E, %) were calculated as follows:

$$E = \left(1 - \frac{C_p}{C_i}\right) \times 100 \tag{1}$$

where C_p and C_i are the permeate and initial heavy metal concentrations (mg/L), respectively.

3.8. Binding isotherm and relative adsorption capacity

The relative adsorption capacity of amyloid fibrils and activated carbon (q) were calculated by the mass difference of heavy metals per mass of adsorbent using the equation:

$$q = \frac{(C_{m,i} - C_{m,p}) \times V}{m} \tag{2}$$

where $C_{m,i}$ and $C_{m,p}$ are the initial and permeate metal ion concentrations (ppb), V is the volume filtered (L), and m is the mass of protein fibrils (mg).

To obtain the different binding isotherms of each protein type with various heavy metals, fixed amounts of amyloid fibrils (7 mg) were incubated with increasing concentrations of each heavy metal ion, to a final volume of 2 mL for 24 h. The solutions were then filtered through a 0.22 μm cellulose membrane and the permeates were collected and analyzed with ICP-OES. The resulting concentrations were plotted against their initial concentrations and modeled with the Swillens and Motulsky fit as shown below:

$$[M \bullet L] = \frac{1}{2}\left([M_0] + [L_0] + \frac{1}{K_a}\right) - \frac{1}{2}\sqrt{\left([M_0] + [L_0] + \frac{1}{K_a}\right)^2 - 4[M_0][L_0]} \tag{3}$$

where [M•L] denotes the metal–ligand concentration, and [M_0], [L_0] and K_a represent the initial metal concentration, the total ligand concentration at saturation, and the binding constant, respectively.

4. Results and discussion

4.1. Protein extraction and isolation

In this study, salt extraction of plant proteins was selected over conventional alkaline extraction due to the possible alteration of protein functionality from the oxidation of phenolic compounds present in the meal under alkaline conditions, which could bind covalently to proteins and negatively affect protein functionality [28,29]. As observed in Fig. 1, the method begins with the salt extraction of proteins from plant meals followed by the concentration of protein salt extracts and eventually protein precipitation in cold water. During the proteins' precipitation, non-proteinaceous components such as phenolic compounds remain in the aqueous phase, leaving mostly plant globulins in the crude protein precipitate. To further enrich the protein fraction, the crude protein was re-extracted with a salt solution and precipitated at acidic pH.

The isolated proteins were analyzed with SDS-PAGE (Fig. 2a), which displayed the characteristic bands of the sunflower and peanut globulins. Under reducing conditions, polypeptides making up the subunits of 11S sunflower and peanut proteins were clearly observed on the SDS-PAGE gel, with acidic and basic polypeptides having MWs between 25 and 40 kDa and 20 kDa, respectively [30–33]. The 65 kDa band in Lane 2r corresponds to the 7S globulin trimeric subunit of peanut proteins. A further analysis of the amino acid composition of sunflower and peanut proteins (Fig. 2b) revealed compositions with a high content of acidic residues (sunflower: 36.6 mol. %, peanut: 35.3 mol. %), followed by other functional groups from basic residues (sunflower: 10.6 mol. %, peanut: 16.0 mol. %), histidine (sunflower: 2.7 mol. %, peanut: 2.3 mol. %), and cysteine (sunflower: 1.4 mol. %, peanut: 1.6 mol.%). This variety of amino acids in sunflower and peanut proteins provides a versatile tool for the binding of heavy metals through electrostatic and metal-coordination interactions, making them attractive candidates for heavy metal removal [9].

4.2. Amyloid fibril formation

Plant-based amyloid fibrils have been reported from several plant proteins, including oat [34], soybean, and zein proteins [35,36]. In this study, sunflower and peanut were used as sources of proteins for amyloid fibrillization. Amyloid fibrils were observed to grow over the course of 6 to 24 h of heat treatment under acidic conditions as verified by AFM (Figure S1 and S2). Protein monomers were observed to form short fibril seeds from 6 h and below 12 h for sunflower and peanut proteins, respectively. The growth phase occurred after 12 h of heating, during which short fibrils elongated into longer fibrils of 1–3 μm in length with fibril diameters ranging 7–14 nm as observed by TEM (Figure S3). Both AFM and TEM showed that sunflower amyloid fibrils are flexible and curly while peanut amyloid fibrils are more rigid and thicker in diameter. While both sunflower and peanut proteins predominantly formed amyloidogenic fibrillar aggregates, round-shaped non-fibrillar aggregates were also detected in the background of the AFM images, which could arise from the second lowest energy state of amorphous aggregates (instead of the lowest energy state of amyloid fibrils [36,37]) or possibly from impurities remaining in the isolate.

To determine the optimal conditions for amyloid fibrillization, thiazole orange was used to monitor the formation of amyloid fibrils over 24 h during heat treatment at 90, 95, and 100 °C (Fig. 2c and e). Maximum fluorescent intensities of sunflower protein solutions increased with increasing temperature, indicating that amyloid fibril formation of sunflower proteins was favored at higher temperatures, forming the most amyloid fibrils at 100 °C. Peanut proteins, on the other hand, exhibited an opposite behavior showing decreasing fluorescent intensities with increasing temperature. Increased formation of larger

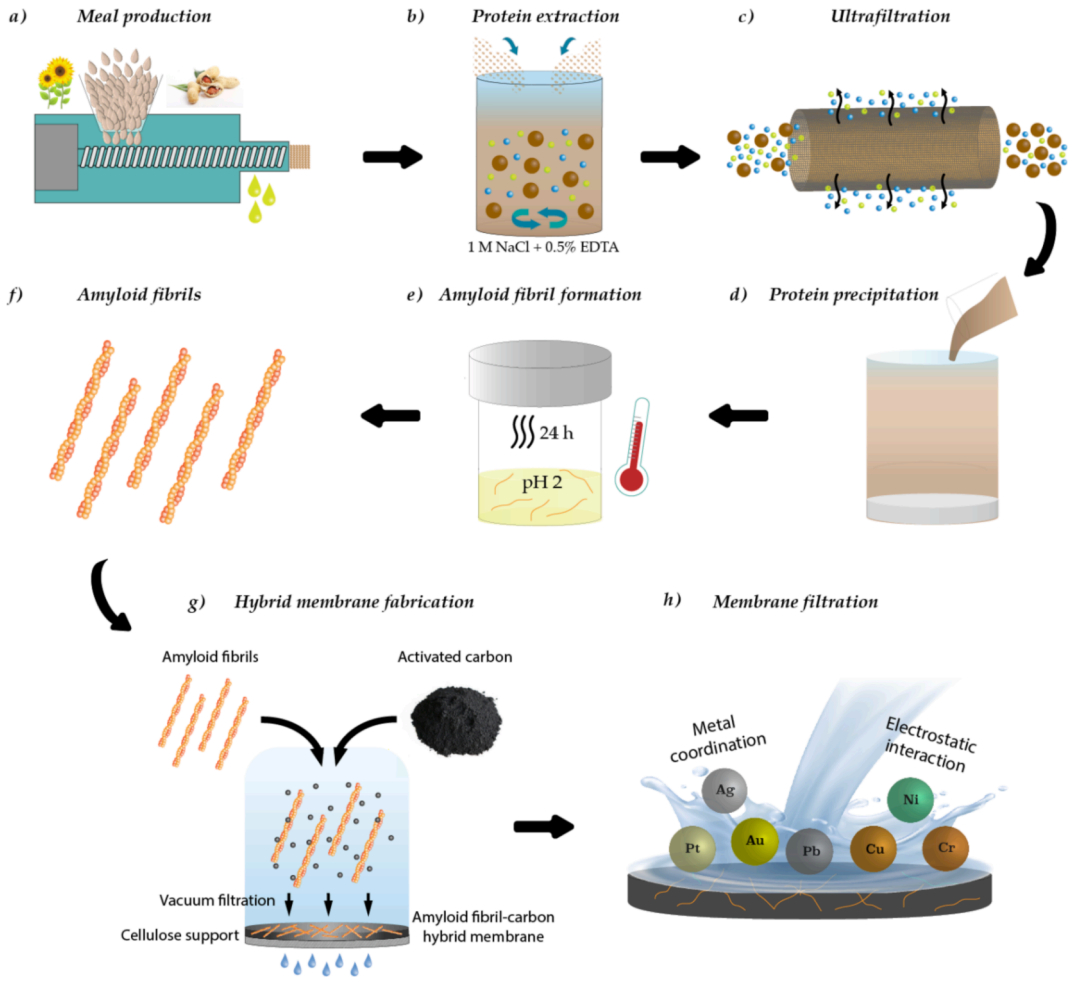

Fig. 1. Schematic of process flow from plant seeds to the amyloid-based filtration membrane. a) Production of sunflower and peanut meals by screw-pressing seeds. b) Aqueous protein extraction of meals (brown spheres: proteins, green spheres: small molecules, blue spheres: water). c) Protein concentration with ultrafiltration. d) Protein precipitation in cold water. e) Plant protein amyloid fibril formation. f) Amyloid fibrils. g) Fabrication of amyloid-carbon hybrid membrane by filtration. h) Heavy metal filtration by plant amyloid-carbon hybrid membranes.

protein aggregates was observed with increasing temperature, which could be due to the less heat resistant 7S globulin protein present in the peanut protein isolate that has earlier been reported to aggregate at 85 °C [38]. This increase in aggregation of 7S globulin at higher temperatures could also suggest the inhibition of amyloid fibril formation of 11S peanut globulins observed from the lower fluorescence intensities. The optimal temperatures for amyloid fibril formation are therefore 100 °C and 90 °C for sunflower and peanut proteins, respectively, with a heat treatment time of 24 h. Sunflower and peanut amyloid fibrils formed in these conditions are shown in Fig. 2d and f, respectively, revealing long fibrils spanning several micrometers.

The insets of Fig. 2d and f show the solutions of sunflower and peanut amyloid fibrils obtained after heat treatment under cross-polarized light, exhibiting the distinct birefringence from the nematic phase of amyloid fibrils[39]. This result was in contrast to that obtained with direct acid precipitation of proteins after salt extraction, where heat-treated protein solutions produced a dark colored turbid solution and did not exhibit distinct birefringence (Figure S4a). Similar observations were also seen when salt-extracted protein solutions were diafiltered with fresh NaCl followed by acid precipitation (Figure S4b). The absence of clear birefringence in direct acid precipitated proteins suggests the presence not only of phenolic compounds, but also of other co-precipitated compounds from plant meals that aggregated or affected amyloid fibril formation upon heat treatment. These compounds were most likely separated and removed when proteins were precipitated by dilution, hence producing clear birefringent amyloid solutions. To the best of our knowledge, this is the first report of amyloid fibrils obtained from sunflower and peanut proteins.

4.3. Heavy metal removal studies

To assess the performance of sunflower and peanut amyloid fibrils for heavy metal removal from wastewater, heavy metal solutions of Pt, Cr, and Pb were filtered using sunflower and peanut amyloid hybrid membranes. Fig. 3a shows the better performance of sunflower and peanut amyloid membranes than pristine activated carbon membranes in removing these heavy metals, achieving 99.76% and 99.86% for Pt, 88.29% and 88.05% for Cr, and 99.36% and 99.40% for Pb, respectively, calculated using equation (1). To investigate the individual performance of sunflower and peanut amyloid fibrils on heavy metal adsorption, pure amyloid fibril membranes were used for filtration of heavy metal solutions and the difference in heavy metal concentrations before and after filtration were used to calculate the heavy metal specific adsorption capacity of the fibrils using equation (2). As a control, the same heavy metal solutions were filtered with pure activated carbon membranes to determine the adsorption capacity of activated carbon (.Fig. 3b).

Amyloid fibrils have been shown to be able to bind to heavy metals due to the variety of amino acid side-chains exposed to the fibril surface after fibrillization [11]. These side-chains mediate heavy metal binding through different intermolecular interactions, including electrostatic

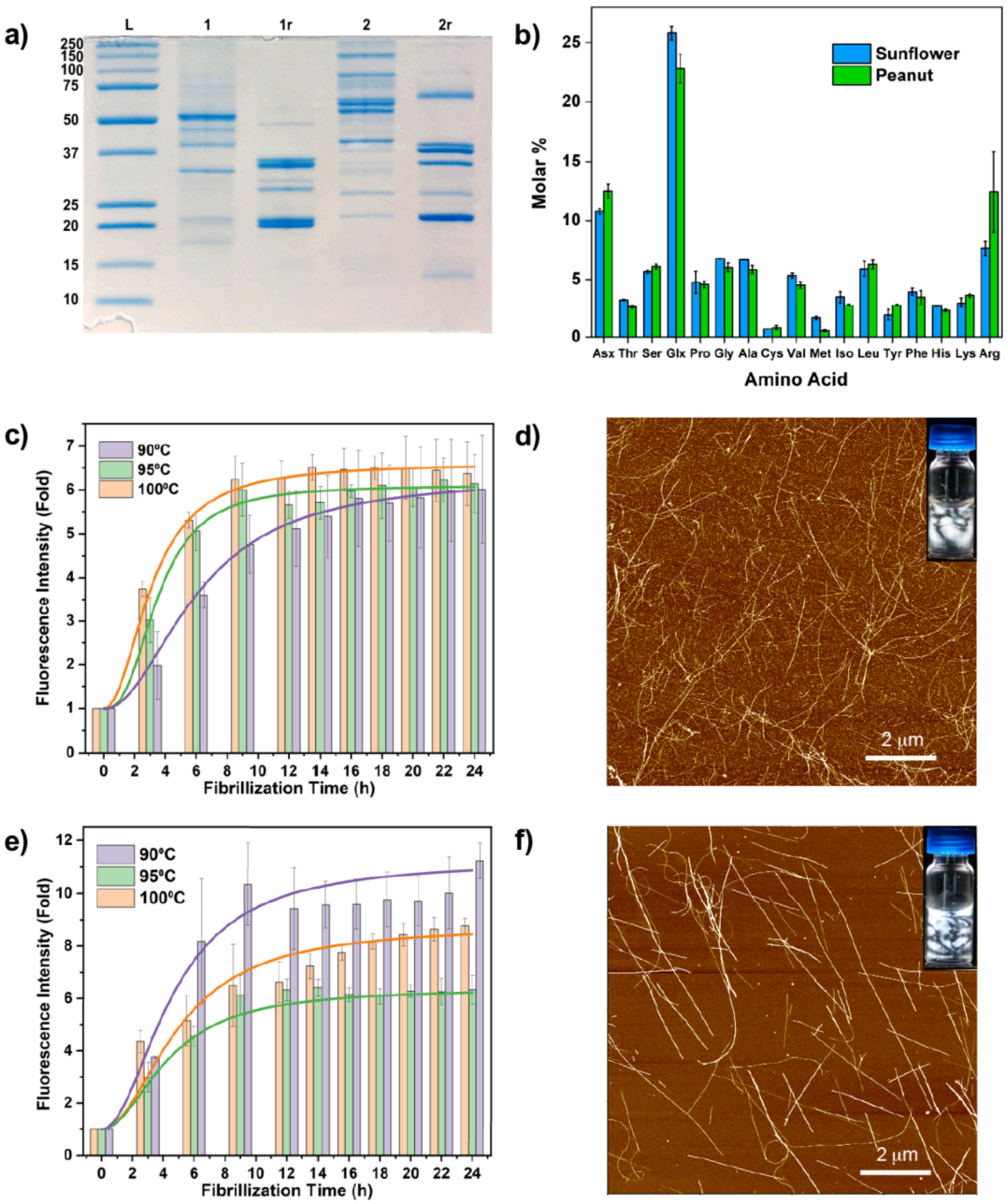

Fig. 2. a) SDS-PAGE of protein isolates. Lane 1: sunflower protein. Lane 1r: sunflower protein reduced. Lane 2: peanut protein. Lane 2r: peanut protein reduced. b) Amino acid profiles of sunflower and peanut protein isolates. c) Fibrillization temperature–time study of sunflower amyloid fibrils. d) AFM images of sunflower amyloid fibrils heat treated at 100 °C for 24 h. Inset: Cross-polarized image of sunflower amyloid fibril solution. e) Fibrillization temperature–time study of peanut amyloid fibrils. f) Peanut amyloid fibrils heat treated at 90 °C for 24 h. Inset: Cross-polarized image of peanut amyloid fibril solution.

interactions and metal chelation [16]. The nature of these heavy metals in addition to the metal species in solution both play a role in ligand–metal binding, as proposed by the Hard Acid Soft Base (HSAB) theory, which is a framework describing different metal ion interactions based on their inherent chemistry [40]. According to the HSAB theory, the 'hardness' of the 3 metals tested in this study can be ranked as: Cr > Pb > Pt. Cr, both in the + 3 and + 6 oxidation states, is classified as a hard acid, Pb is classified as a borderline to soft acid, whereas Pt is a soft acid.

The heavy metal specific adsorption capacities per mg of sunflower and peanut amyloid fibrils were determined to be at least twice or higher than those of activated carbon, demonstrating the heavy metal binding capability of plant fibrils (Fig. 3b). This was further demonstrated with gold (Au), silver (Ag), nickel (Ni), and copper (Cu) solutions (Figure S5). The relative adsorption capacities of sunflower and peanut amyloid fibrils for these metallic ions were also measured to be more than twice the capacity compared to activated carbon, demonstrating the wide applicability of heavy metal adsorption of plant amyloid fibrils. Across the heavy metals studied, amyloid fibrils possessed higher adsorption capacities towards the softer metals Pt, Au, and Ag compared to the harder metals Cr, Ni, and Cu. As softer metals tend to bind through metal coordination while harder metals bind through electrostatic interactions, the presence of softer thiol functional groups from cysteine likely provided an additional capability to bind Pt, Au, and Ag. Fitted parameters based on equation (3) obtained from heavy metal binding isotherms of sunflower and peanut amyloid fibrils for Pt, Cr, and Pb (Figure S6) showed the highest binding constants for Pt, whereas higher saturation limits were obtained for Cr and Pb. The binding of metal to

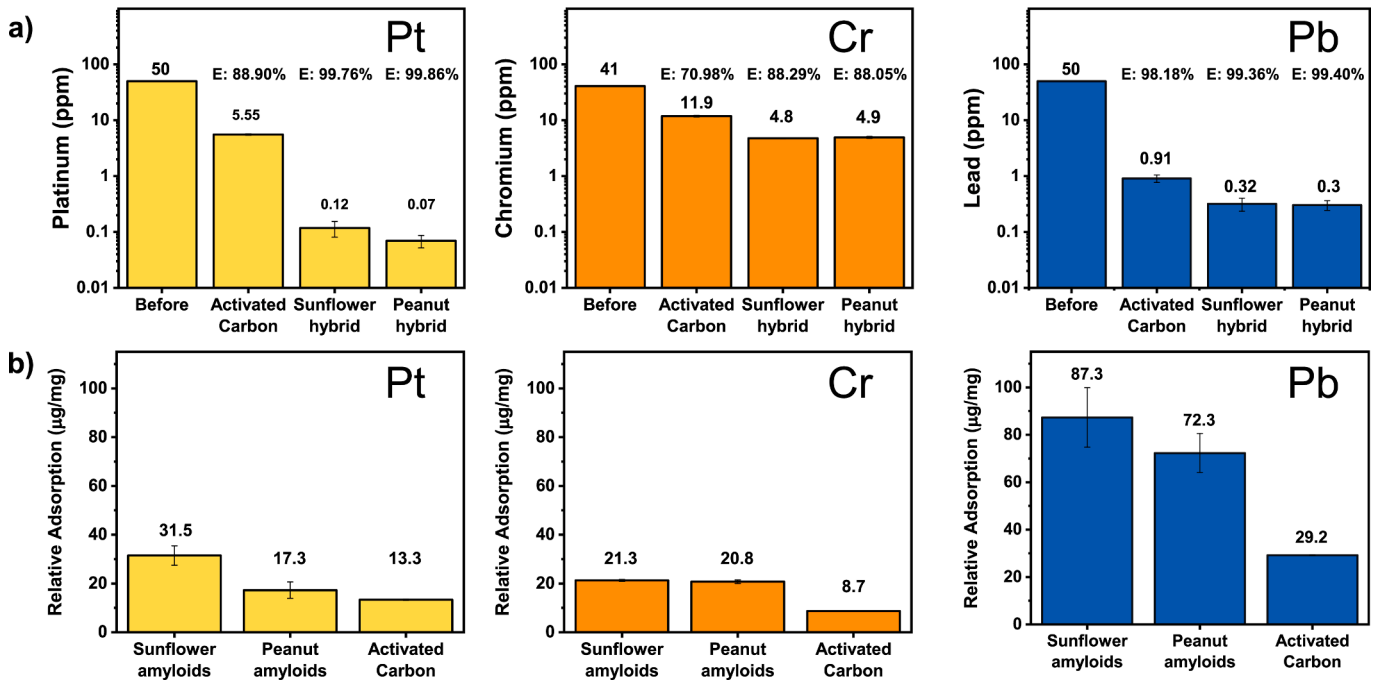

Fig. 3. a) Filtration of pristine activated carbon, sunflower and peanut amyloid-carbon hybrid membranes of Pt, Cr, and Pb. b) Comparison of relative adsorption capacities of sunflower amyloid fibrils, peanut amyloid fibrils, and activated carbon. E: removal efficiency (%).

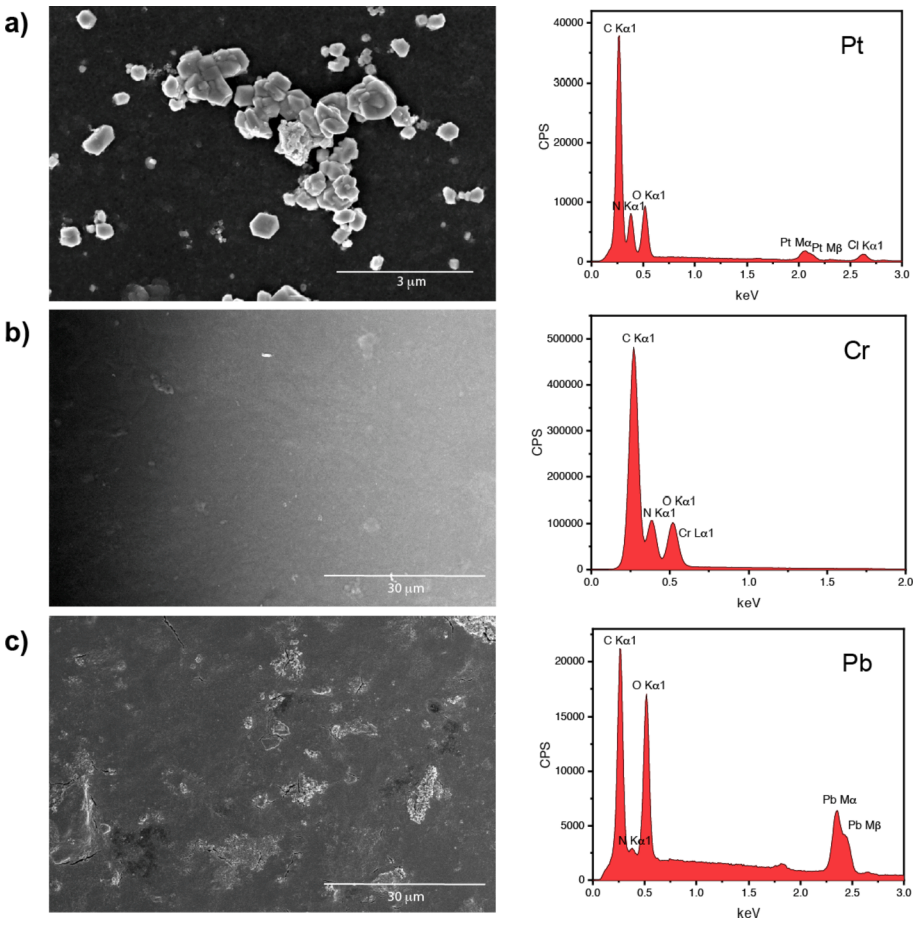

Fig. 4. SEM images of pure sunflower amyloid fibrils membranes filtered with a) Pt; b) Cr; and c) Pb and their respective EDX spectra.

amino acids, however, is a complex phenomenon, which could also depend on sequence motifs with specific metal-binding pockets [41].

Membranes containing only amyloid fibrils filtered with the respective heavy metals were further analyzed by SEM equipped with an EDX detector. As seen in Fig. 4, Pt crystals with sizes ranging between 300 and 500 nm were observed on the surface of the Pt-filtered membrane, while the Pb-filtered membrane showed the presence of small aggregates. The Cr-filtered membrane exhibited the smoothest surface among the 3 membranes. EDX analysis performed across the surface of the membranes displayed the characteristic peaks of each heavy metal, namely Pt *Mα* at 2.05 keV, Cr *Lα* at 0.6 keV, and Pb *Mα* at 2.3 keV, which confirmed the adsorption of heavy metals onto the surface of amyloid fibrils. This was supported by an elemental map of the Pt-filtered membrane surface showing the adsorption of Pt across the membrane surface (Figure S7). Within the operating voltage used, the Pt and Pb characteristic peaks are notably distinct from the C, N, and O peaks due to their much larger atomic number, while the peak of Cr was observed to overlap with O.

To assess the applicability of the hybrid membranes in turning polluted wastewater into water of drinkable standards, heavy metal concentrations in the ppb range were used as simulated wastewater. When filtering 100 mL of heavy metal solutions (initial concentration of *ca.* 400–520 ppb) over 10 cycles through a 10 wt% amyloid-carbon membrane, removal efficiencies of Pt (Figs. 5a and 5d) and Pb (Figs. 5c and 5f) remained more than 99% throughout the 10 cycles, having yet to show signs of saturation. Moreover, Pb concentrations in the filtrate were well below 10 ppb, fulfilling the WHO threshold limit for drinking water. These results indicate that the plant amyloid-carbon membranes containing only 6.7 mg of protein are able to process wastewater into drinkable water, after which the low cost membranes can be simply disposed without further regeneration or desorption. Cr removal by hybrid membranes was, however, less satisfactory (Figs. 5b and 5e), achieving more than 90% removal efficiencies for the first 3 cycles but decreasing thereafter, insufficiently removing Cr ions below the WHO permissible limit of 50 ppb.

One possible reason for the poorer adsorption behavior of Cr could be explained with the HSAB theory. The adsorption of metal ions on activated carbon has been shown to depend on the molecular structure of activated carbon made up of basal structural units (BSUs). The presence of oxygen groups on the edge of the BSUs makes it a hard site, while surface aromatic sheets are soft sites[42]. The ratio of sites then depends on the processing involved in the production of activated carbon. Comparison of the measured relative adsorption capacities of activated carbon of all 7 metals tested (Pt, Cr, and Pb in Fig. 3, and Au, Ag, Ni, and

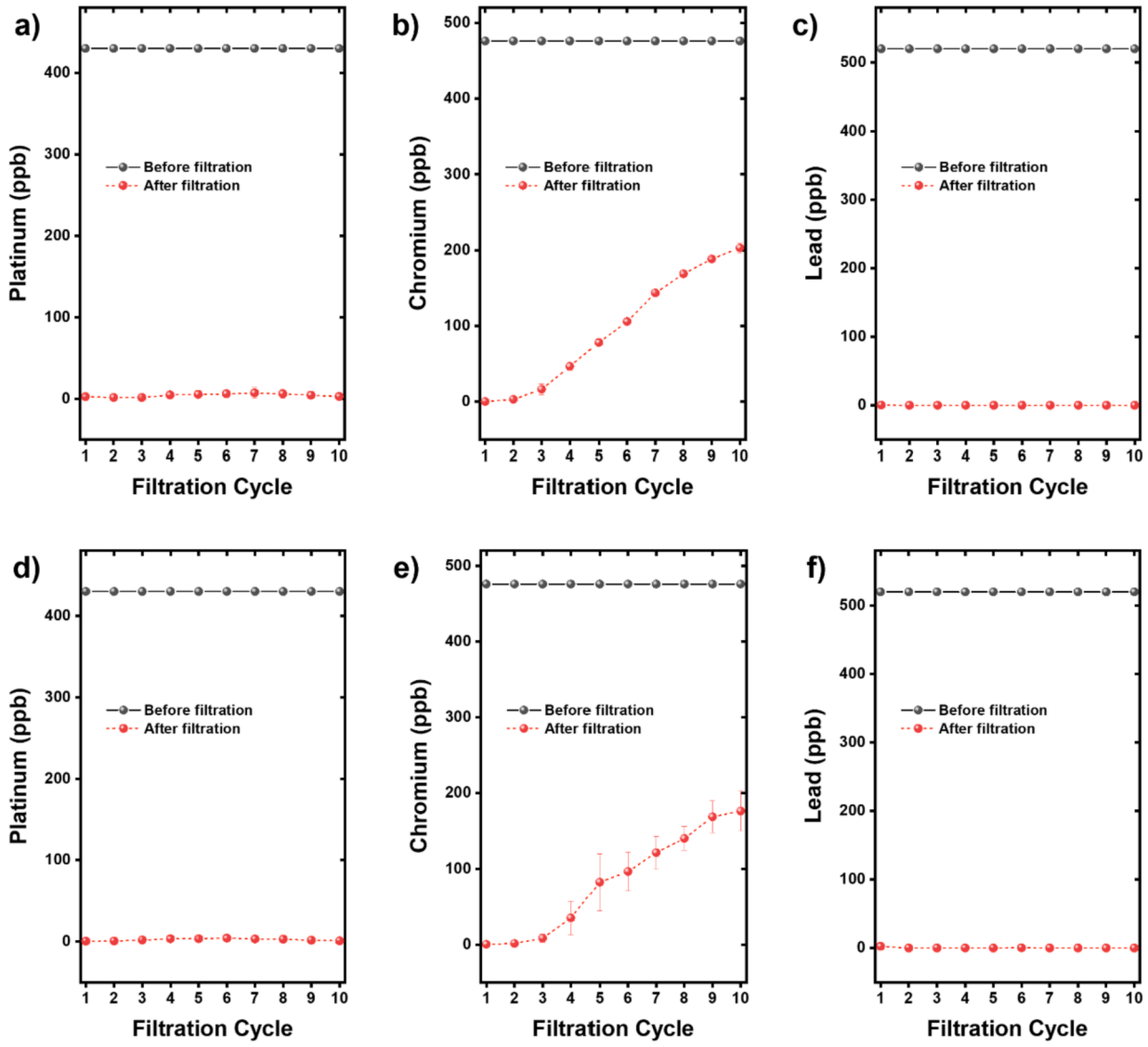

Fig. 5. Performance of plant amyloid-carbon hybrid membranes over multiple filtration cycles. a) Sunflower: Pt. b) Sunflower: Cr. c) Sunflower: Pb. d) Peanut: Pt. e) Peanut: Cr. f) Peanut: Pb.

Cu in Figure S5) shows that the adsorption capacities of activated carbon for harder acids Cr, Ni, and Cu were smaller than those of softer acids Pt, Au, Ag, and Pb. This implies that the activated carbon used in this study most likely possessed more soft sites than hard sites, which could result in overall weaker metal binding strength for hard acids. As also seen from the positive contribution of amyloid fibrils in heavy metal removal in Fig. 3, the lower performance of Cr removal could hence be due to the weaker adsorption of Cr by activated carbon instead of protein amyloids, although further studies will be required to validate this suggestion.

5. Conclusion

A green and sustainable process of extracting and isolating sunflower and peanut proteins from oilseed meals that were subsequently self-assembled into amyloid fibrils was developed. Plant amyloid fibrils were further used to fabricate plant amyloid-carbon hybrid membranes that were assessed for their heavy metal adsorption capabilities. Both sunflower and peanut amyloid fibrils exhibited higher heavy metal adsorption capacities than activated carbon for a variety of heavy metals. Pt, Cr, and Pb were chosen as target heavy metal pollutants to demonstrate that wastewater could be turned into drinking water. Both sunflower and peanut amyloids displayed high removal efficiencies of Pt and Pb over several consecutive cycles of filtration, achieving concentrations below the WHO permissible limits for drinking water. Altogether, this study indicates the versatility of turning low-cost proteins from food waste into amyloid fibrils for treating heavy metal polluted water into clean drinkable water. The process should be readily scalable due to its simplicity and minimal use of chemical reagents, pointing towards sustainable and low-cost water treatment technologies.

Declaration of Competing Interest

The authors declare that they have no known competing financial interests or personal relationships that could have appeared to influence the work reported in this paper.

Acknowledgments

This research was supported by the strategic initiative on biomimetic and sustainable materials (IBSM), Nanyang Technological University (NTU), Singapore. W.L.S thanks NTU Singapore for a Nanyang President Graduate Scholarship (NPGS). The authors acknowledge the support of Dr. Anne Greet Bittermann and Stephan Handschin of ScopeM/ETH Zurich.

Appendix A. Supplementary data

Supplementary data to this article can be found online at https://doi.org/10.1016/j.cej.2022.136513.

References

[1] S. Bolisetty, M. Peydayesh, R. Mezzenga, Sustainable technologies for water purification from heavy metals: review and analysis, Chem. Soc. Rev. 48 (2) (2019) 463–487, https://doi.org/10.1039/C8CS00493E.
[2] F. Fu, Q. Wang, Removal of heavy metal ions from wastewaters: A review, J. Environ. Manage. 92 (3) (2011) 407–418, https://doi.org/10.1016/j.jenvman.2010.11.011.
[3] M.A. Barakat, New trends in removing heavy metals from industrial wastewater, Arabian J. Chem. 4 (4) (2011) 361–377, https://doi.org/10.1016/j.arabjc.2010.07.019.
[4] N.A.A. Qasem, R.H. Mohammed, D.U. Lawal, Removal of heavy metal ions from wastewater: a comprehensive and critical review, npj Clean Water 4 (1) (2021) 36, https://doi.org/10.1038/s41545-021-00127-0.
[5] T.S. Vo, M.M. Hossain, H.M. Jeong, K. Kim, Heavy metal removal applications using adsorptive membranes, Nano Convergence 7 (1) (2020) 36, https://doi.org/10.1186/s40580-020-00245-4.
[6] R. Ghahremani, B. Baheri, M. Peydayesh, S. Asarehpour, T. Mohammadi, Novel crosslinked and zeolite-filled polyvinyl alcohol membrane adsorbents for dye removal, Res. Chem. Intermed. 41 (12) (2015) 9845–9862, https://doi.org/10.1007/s11164-015-1988-3.
[7] A. Gupta, V. Sharma, K. Sharma, V. Kumar, S. Choudhary, P. Mankotia, B. Kumar, H. Mishra, A. Moulick, A. Ekielski, P.K. Mishra, A review of adsorbents for heavy metal decontamination: growing approach to wastewater treatment, Materials (Basel) 14 (16) (2021) 4702, https://doi.org/10.3390/ma14164702.
[8] M. Bilal, I. Ihsanullah, M. Younas, M. Ul Hassan Shah, Recent advances in applications of low-cost adsorbents for the removal of heavy metals from water: a critical review, Sep. Purif. Technol. 278 (2021) 119510, https://doi.org/10.1016/j.seppur.2021.119510.
[9] M.M. Yamashita, L. Wesson, G. Eisenman, D. Eisenberg, Where metal ions bind in proteins, Proc. Natl. Acad. Sci. 87 (15) (1990) 5648, https://doi.org/10.1073/pnas.87.15.5648.
[10] S. Bolisetty, R. Mezzenga, Amyloid–carbon hybrid membranes for universal water purification, Nat. Nanotechnol. 11 (4) (2016) 365–371, https://doi.org/10.1038/nnano.2015.310.
[11] M. Peydayesh, S. Bolisetty, T. Mohammadi, R. Mezzenga, Assessing the binding performance of amyloid-carbon membranes toward heavy metal ions, Langmuir 35 (11) (2019) 4161–4170, https://doi.org/10.1021/acs.langmuir.8b04234.
[12] S. Bolisetty, N. Reinhold, C. Zeder, M.N. Orozco, R. Mezzenga, Efficient purification of arsenic-contaminated water using amyloid–carbon hybrid membranes, Chem. Commun. 53 (42) (2017) 5714–5717, https://doi.org/10.1039/C7CC00406K.
[13] M. Peydayesh, M. Pauchard, S. Bolisetty, F. Stellacci, R. Mezzenga, Ubiquitous aluminium contamination in water and amyloid hybrid membranes as a sustainable possible solution, Chem. Commun. 55 (74) (2019) 11143–11146, https://doi.org/10.1039/C9CC05337A.
[14] Q. Zhang, S. Zhang, Z. Zhao, M. Liu, X. Yin, Y. Zhou, Y. Wu, Q. Peng, Highly effective lead (II) removal by sustainable alkaline activated β-lactoglobulin nanofibrils from whey protein, J. Cleaner Prod. 255 (2020), 120297, https://doi.org/10.1016/j.jclepro.2020.120297.
[15] L.C. Ramírez-Rodríguez, L.E. Díaz Barrera, M.X. Quintanilla-Carvajal, D. I. Mendoza-Castillo, A. Bonilla-Petriciolet, C. Jiménez-Junca, Preparation of a hybrid membrane from whey protein fibrils and activated carbon to remove mercury and chromium from water, Membranes 10 (12) (2020), https://doi.org/10.3390/membranes10120386.
[16] M. Peydayesh, R. Mezzenga, Protein nanofibrils for next generation sustainable water purification, Nat. Commun. 12 (1) (2021) 3248, https://doi.org/10.1038/s41467-021-23388-2.
[17] G.V. Research, Whey Protein Market Size, Share & Trends Analysis Report By Type (Whey Protein Isolates, Whey Protein Concentrates, Whey Protein Hydrolysates), By Application, By Region, And Segment Forecasts, 2020 - 2027, 2020. https://www.grandviewresearch.com/industry-analysis/whey-protein-market.
[18] D. Liu, Z. Li, W. Li, Z. Zhong, J. Xu, J. Ren, Z. Ma, Adsorption behavior of heavy metal ions from aqueous solution by soy protein hollow microspheres, Ind. Eng. Chem. Res. 52 (32) (2013) 11036–11044, https://doi.org/10.1021/ie401092f.
[19] J. Liu, D. Su, J. Yao, Y. Huang, Z. Shao, X. Chen, Soy protein-based polyethylenimine hydrogel and its high selectivity for copper ion removal in wastewater treatment, J. Mater. Chem. A 5 (8) (2017) 4163–4171, https://doi.org/10.1039/C6TA10814H.
[20] H.-F. Wen, C. Yang, D.-G. Yu, X.-Y. Li, D.-F. Zhang, Electrospun zein nanoribbons for treatment of lead-contained wastewater, Chem. Eng. J. 290 (2016) 263–272, https://doi.org/10.1016/j.cej.2016.01.055.
[21] R. Shukla, M. Cheryan, Zein: the industrial protein from corn, Ind. Crops Prod. 13 (3) (2001) 171–192, https://doi.org/10.1016/S0926-6690(00)00064-9.
[22] J. Pedroche, 13 - Utilization of Sunflower Proteins, in: E. Martínez-Force, N.T. Dunford, J.J. Salas (Eds.), Sunflower, AOCS Press2015, pp. 395-439. doi:10.1016/B978-1-893997-94-3.50019-2.
[23] C.P. Duodu, D. Adjei-Boateng, R.E. Edziyie, N.W. Agbo, G. Owusu-Boateng, B. K. Larsen, P.V. Skov, Processing techniques of selected oilseed by-products of potential use in animal feed: effects on proximate nutrient composition, amino acid profile and antinutrients, Anim. Nutr. 4 (4) (2018) 442–451, https://doi.org/10.1016/j.aninu.2018.05.007.
[24] J.P.D. Wanasundara, Proteins of brassicaceae oilseeds and their potential as a plant protein source, Crit. Rev. Food Sci. Nutr. 51 (7) (2011) 635–677, https://doi.org/10.1080/10408391003749942.
[25] U.S.D.o.A.F.A. Service, Oilseeds: World Markets and Trade, 2021. https://apps.fas.usda.gov/psdonline/circulars/oilseeds.pdf.
[26] G.-Q. Gao, A.-W. Xu, A new fluorescent probe for monitoring amyloid fibrillation with high sensitivity and reliability, RSC Adv. 3 (43) (2013) 21092–21098, https://doi.org/10.1039/C3RA43259A.
[27] Y. Shen, L. Posavec, S. Bolisetty, F.M. Hilty, G. Nyström, J. Kohlbrecher, M. Hilbe, A. Rossi, J. Baumgartner, M.B. Zimmermann, R. Mezzenga, Amyloid fibril systems reduce, stabilize and deliver bioavailable nanosized iron, Nat. Nanotechnol. 12 (7) (2017) 642–647, https://doi.org/10.1038/nnano.2017.58.
[28] S.R. Wildermuth, E.E. Young, L.M. Were, Chlorogenic acid oxidation and its reaction with sunflower proteins to form green-colored complexes, Compr. Rev. Food Sci. Food Saf. 15 (5) (2016) 829–843, https://doi.org/10.1111/1541-4337.12213.
[29] M. Saeed, M. Cheryan, Chlorogenic acid interactions with sunflower proteins, J. Agric. Food. Chem. 37 (5) (1989) 1270–1274, https://doi.org/10.1021/jf00089a015.
[30] S. González-Pérez, Physico-chemical and functional properties of sunflower proteins, (2003).

[31] S. González-Pérez, 12 - Sunflower Proteins, in: E. Martínez-Force, N.T. Dunford, J. J. Salas (Eds.), Sunflower, AOCS Press, 2015, pp. 331–393, https://doi.org/10.1016/B978-1-893997-94-3.50018-0.
[32] S. González-Pérez, J.M. Vereijken, Sunflower proteins: overview of their physicochemical, structural and functional properties, J. Sci. Food Agric. 87 (12) (2007) 2173–2191, https://doi.org/10.1002/jsfa.2971.
[33] L. Wang, H. Liu, L. Liu, Q. Wang, Q. Li, Y. Du, J. Zhang, Protein contents in different peanut varieties and their relationship to gel property, Int. J. Food Prop. 17 (7) (2014) 1560–1576, https://doi.org/10.1080/10942912.2012.723660.
[34] J. Zhou, T. Li, M. Peydayesh, M. Usuelli, V. Lutz-Bueno, J. Teng, L. Wang, R. Mezzenga, Oat Plant Amyloids for Sustainable Functional Materials, Advanced Science n/a(n/a) (2021) 2104445. doi:10.1002/advs.202104445.
[35] A. Herneke, C. Lendel, D. Johansson, W. Newson, M. Hedenqvist, S. Karkehabadi, D. Jonsson, M. Langton, Protein nanofibrils for sustainable food-characterization and comparison of fibrils from a broad range of plant protein isolates, ACS Food Sci. Technol. 1 (5) (2021) 854–864, https://doi.org/10.1021/acsfoodscitech.1c00034.
[36] Y. Cao, R. Mezzenga, Food protein amyloid fibrils: origin, structure, formation, characterization, applications and health implications, Adv. Colloid Interface Sci. 269 (2019) 334–356, https://doi.org/10.1016/j.cis.2019.05.002.
[37] P.C. Ke, R. Zhou, L.C. Serpell, R. Riek, T.P.J. Knowles, H.A. Lashuel, E. Gazit, I. W. Hamley, T.P. Davis, M. Fändrich, D.E. Otzen, M.R. Chapman, C.M. Dobson, D. S. Eisenberg, R. Mezzenga, Half a century of amyloids: past, present and future, Chem. Soc. Rev. 49 (15) (2020) 5473–5509, https://doi.org/10.1039/C9CS00199A.
[38] R.Y.Y. Chiou, Effects of heat treatments on peanut arachin and conarachin, J. Food Biochem. 14 (3) (1990) 219–232, https://doi.org/10.1111/j.1745-4514.1990.tb00835.x.
[39] B. Hu, Y. Shen, J. Adamcik, P. Fischer, M. Schneider, M.J. Loessner, R. Mezzenga, Polyphenol-binding amyloid fibrils self-assemble into reversible hydrogels with antibacterial activity, ACS Nano 12 (4) (2018) 3385–3396, https://doi.org/10.1021/acsnano.7b08969.
[40] R.G. Pearson, Hard and soft acids and bases, HSAB, part 1: Fundamental principles, J. Chem. Educ. 45 (9) (1968) 581, https://doi.org/10.1021/ed045p581.
[41] A. Stank, D.B. Kokh, J.C. Fuller, R.C. Wade, Protein Binding Pocket Dynamics, Acc. Chem. Res. 49 (5) (2016) 809–815, https://doi.org/10.1021/acs.accounts.5b00516.
[42] A. Alfarra, E. Frackowiak, F. Béguin, The HSAB concept as a means to interpret the adsorption of metal ions onto activated carbons, Appl. Surf. Sci. 228 (1) (2004) 84–92, https://doi.org/10.1016/j.apsusc.2003.12.033.